The influence of edge viscosity on plasma instabilities

G.O. Ludwig

Associated Plasma Laboratory, National Space Research Institute
12227-010, São José dos Campos, SP, Brazil

e-mail: ludwig@plasma.inpe.br

Abstract. Viscous stresses may be important in the behavior of natural and laboratory plasmas. This paper examines two cases where edge viscosity affects the shape and level of instabilities in plasma discharges. These simple models are developed in the framework of the hydromagnetic equations, including viscosity effects though considering the plasma as a perfectly conducting fluid.

1. Introduction

The interface between the plasma and its surroundings affects both the structure of plasma instabilities and the quality of confinement. According to well established procedures in magnetohydrodynamic (MHD) theory, the boundary conditions for the analysis of instabilities is set by the flow of mass, magnetic flux, and energy across the boundary. However, ideal MHD disregards the role of viscosity in fluid motion. Although viscosity effects can be generally neglected in the study of large scale instabilities in fusion plasmas, they may have a strong influence on high order modes of oscillation near the plasma edge.

This paper reports two instances where edge viscosity has a significant role. In the first example the turbulence associated with the Rayleigh-Taylor instability, which is driven during the contraction stage of the decaying return stroke of a lightning discharge, creates anomalous viscosity that defines the spatial structure of bead lightning. In the second example the high beta current driven instabilities in a cylindrical plasma are examined by taking into account the effect of viscosity at the boundary. It is shown that the $m = 1$ kink mode is barely changed, but the higher order $m \geq 2$ modes are significantly damped by high edge viscosity (low collisionality). This has interesting implications for magnetic fusion, since the ballooning modes, which set a limit to the maximum pressure that can be confined in a tokamak, could be strongly affected. In the presence of flow at the edge (not considered here) viscous stresses are expected to modify the stability conditions, acting as a "surface tension".

2. Formulation of the hydromagnetic problem

The problems examined in this paper are described by the fluid equations for a viscous magnetized plasma [1, 2, 3]. These are the mass conservation equation, Navier-Stokes equation, local equation of state, Ampère's law, and combined Faraday's and Ohm's laws for a perfectly conductive fluid, given respectively by

$$\begin{aligned}
\frac{\partial \rho}{\partial t} + \nabla \cdot (\rho \overrightarrow{v}) &= 0, \\
\rho \frac{d \overrightarrow{v}}{dt} &= -\nabla p + \overrightarrow{j} \times \overrightarrow{B} + \eta \nabla^2 \overrightarrow{v} + \frac{1}{3} \eta \nabla \left(\nabla \cdot \overrightarrow{v} \right) + \rho \overrightarrow{g}, \\
\frac{d}{dt} \left(\frac{p}{\rho^\gamma} \right) &= 0, \\
\nabla \times \overrightarrow{B} &= \mu_0 \overrightarrow{j}, \\
\frac{\partial \overrightarrow{B}}{\partial t} &= \nabla \times \left(\overrightarrow{v} \times \overrightarrow{B} \right),
\end{aligned} \tag{1}$$

where η is the coefficient of shear viscosity and $\overrightarrow{g}$ models a localized acceleration field.

A set of appropriate boundary conditions is specified by the continuity of the magnetic field in the absence or presence of a surface current density $\overrightarrow{K}$, fluid continuity, no-slip, stress continuity, and pressure balance conditions, given respectively by

$$\begin{array}{c} \left\langle \widehat{n}\cdot\overrightarrow{B}\right\rangle =0\quad\text{if}\quad\overrightarrow{K}=0\quad\text{or}\quad\widehat{n}\cdot\left[\overrightarrow{B}\right]_{a}=0\quad\text{if}\quad\overrightarrow{K}\neq0\ ,\\ \left\langle \widehat{n}\cdot\overrightarrow{v}\right\rangle =0\quad,\quad\left\langle \eta\widehat{n}\times\overrightarrow{v}\right\rangle =0\ ,\\ \left\langle \eta\widehat{n}\times\left[\widehat{n}\cdot\left(\nabla\overrightarrow{v}\right)+\left(\nabla\overrightarrow{v}\right)\cdot\widehat{n}\right]\right\rangle =0,\\ \left\langle p+\overline{\rho}\left(a\right)\phi_{g}+\frac{B^{2}}{2\mu_{0}}-2\eta\widehat{n}\cdot\left(\nabla\overrightarrow{v}\right)\cdot\widehat{n}+\frac{2}{3}\eta\nabla\cdot\overrightarrow{v}\right\rangle =0, \end{array} \tag{2}$$

where $\overline{\rho}\left(a\right)$ is an average mass density at the edge and the "gravitational" potential ϕ_g is related to the acceleration by $\overrightarrow{g}=-\nabla\phi_{g}$.

The equilibrium equations with negligible flow, which is the standard assumption in static ideal MHD, are:

$$\begin{array}{rclcrcl} \nabla p & = & \overrightarrow{j}\times\overrightarrow{B}+\rho\overrightarrow{g} & , & \nabla\times\overrightarrow{B} & = & \mu_{0}\overrightarrow{j},\\ \nabla\cdot\overrightarrow{B} & = & 0 & , & \overrightarrow{v} & = & 0. \end{array} \tag{3}$$

Stability of the fluid equilibrium is tested expressing the perturbation in the velocity in terms of a Lagrangian displacement

$$\delta\overrightarrow{v}=\partial\overrightarrow{\xi}/\partial t=-i\omega\overrightarrow{\xi}. \tag{4}$$

The equation of motion for the perturbations is

$$\begin{array}{rcl} -\rho\omega^{2}\overrightarrow{\xi}-\frac{1}{\mu_{0}}\overrightarrow{B}\cdot\delta\overrightarrow{B} & = & -\nabla\delta p^{*}-\underbrace{i\omega\eta\frac{4}{3}\nabla\left(\nabla\cdot\overrightarrow{\xi}\right)}_{\text{compressive term}}-\overrightarrow{g}\nabla\cdot\left(\rho\overrightarrow{\xi}\right)\\ & & +\frac{1}{\mu_{0}}\delta\overrightarrow{B}\cdot\nabla\overrightarrow{B}+\underbrace{i\omega\eta\nabla\times\left(\nabla\times\overrightarrow{\xi}\right)}_{\text{induced vorticity}}, \end{array} \tag{5}$$

where the total perturbed pressure is

$$\delta p^{*}=\delta p+\frac{\overrightarrow{B}}{\mu_{0}}\cdot\delta\overrightarrow{B}=\underbrace{-\overrightarrow{\xi}\cdot\nabla p-\gamma p\nabla\cdot\overrightarrow{\xi}}_{\text{compressive perturbation}}+\frac{\overrightarrow{B}}{\mu_{0}}\cdot\delta\overrightarrow{B}, \tag{6}$$

and the internal magnetic field perturbation is

$$\delta\overrightarrow{B}=\nabla\times\left(\overrightarrow{\xi}\times\overrightarrow{B}\right)=\underbrace{-\overrightarrow{B}\left(\nabla\cdot\overrightarrow{\xi}\right)}_{\text{compressive term}}+\left(\overrightarrow{B}\cdot\nabla\right)\overrightarrow{\xi}-\left(\overrightarrow{\xi}\cdot\nabla\right)\overrightarrow{B}. \tag{7}$$

The external magnetic field perturbation is given in terms of a magnetic potential ϕ_m by

$$\delta\overrightarrow{B}=-\mu_{0}\nabla\phi_{m}. \tag{8}$$

The boundary conditions for the perturbations are specified by the continuity of the magnetic field (in the presence of a surface current), fluid continuity, no-slip, stress continuity,

and pressure balance conditions, given respectively by

$$\begin{gathered}
\widehat{n}\cdot\left[\delta\overrightarrow{B}-\nabla\times\left(\overrightarrow{\xi}\times\overrightarrow{B}\right)\right]_{a}=0\quad\text{if}\quad\overrightarrow{K}\neq0,\\
\left\langle\widehat{n}\cdot\overrightarrow{\xi}\right\rangle=0\quad,\quad\left\langle\eta\widehat{n}\times\overrightarrow{\xi}\right\rangle=0,\\
\left\langle\eta\widehat{n}\times\left[\widehat{n}\cdot\left(\nabla\overrightarrow{\xi}\right)+\left(\nabla\overrightarrow{\xi}\right)\cdot\widehat{n}\right]\right\rangle=0,\\
\left\langle\delta p^{*}+\overrightarrow{\xi}\cdot\nabla p-\underbrace{\left(\overline{\rho}\left(a\right)\phi_{g}+\frac{2}{3}i\omega\eta\right)\nabla\cdot\overrightarrow{\xi}}_{\text{compressive term}}-\overline{\rho}\left(a\right)\overrightarrow{\xi}\cdot\overrightarrow{g}+\left(\overrightarrow{\xi}\cdot\nabla\right)\frac{B^{2}}{2\mu_{0}}\right.\\
\left.+i2\omega\eta\widehat{n}\cdot\left(\nabla\overrightarrow{\xi}\right)\cdot\widehat{n}\right\rangle=0.
\end{gathered}\tag{9}$$

In its full form, the equation of motion (5) requires the solution of a boundary layer problem. However, for weak viscosity and relatively low frequency perturbations, vorticity will be slowly generated and can be neglected in a first approximation. Furthermore, one may neglect the small modification introduced by the viscous forces on the energy required to compress the fluid, reducing the equation of motion to the standard MHD form

$$-\rho\omega^{2}\overrightarrow{\xi}-\frac{1}{\mu_{0}}\overrightarrow{B}\cdot\delta\overrightarrow{B}\cong-\nabla\delta p^{*}-\overrightarrow{g}\nabla\cdot\left(\rho\overrightarrow{\xi}\right)+\frac{1}{\mu_{0}}\delta\overrightarrow{B}\cdot\nabla\overrightarrow{B}.\tag{10}$$

Of course, the solution of the equation of motion in this form cannot satisfy the tangential conditions of continuity of the fluid velocity and stress across the boundary layer. Nevertheless, for free-boundary perturbations the most important contribution of the viscosity comes from the normal pressure balance condition

$$\left\langle\delta p^{*}+\overrightarrow{\xi}\cdot\nabla p-\overline{\rho}\left(a\right)\overrightarrow{\xi}\cdot\overrightarrow{g}+\left(\overrightarrow{\xi}\cdot\nabla\right)\frac{B^{2}}{2\mu_{0}}+\underbrace{i2\omega\eta\widehat{n}\cdot\left(\nabla\overrightarrow{\xi}\right)\cdot\widehat{n}}_{\text{damping}}\right\rangle\cong0,\tag{11}$$

where the small contributions in the compressive energy introduced both by the acceleration and the viscous forces across the boundary layer were also neglected.

Finally, the perturbations that retain cylindrical symmetry are of the form

$$\overrightarrow{\xi}=\left[\xi_{r}\left(r\right)\widehat{r}+\xi_{\theta}\left(r\right)\widehat{\theta}+\xi_{z}\left(r\right)\widehat{z}\right]\exp\left(im\theta+ikz-i\omega t\right).\tag{12}$$

3. Natural plasma: bead lightning formation

The first example in this paper proposes a mechanism for the formation of bead lightning, a not well understood phenomenon usually observed in triggered lightning experiments [4]. Figure 1 shows a sequence of pictures taken at 1,000 frames per second corresponding to the slow cooling stage of the lightning discharge channel between two consecutive strokes of a 10-stroke flash. This 45 kA peak current discharge was triggered by a small rocket carrying a thin copper wire connected to the launching platform. The beaded structure in this picture has a characteristic axial wavelength of about 0.5 m estimated from the size of the launching platform also seen in some of the frames. Figure 2 displays the typical current waveform for such a 45 kA triggered discharge.

The lightning discharge is unstable to the sausage ($m = 0$) and kink ($m = 1$) hydromagnetic current driven modes [5]. Also, the hydrodynamic Rayleigh-Taylor instability is driven by the backflow of air into the channel during the contraction stage of the decaying

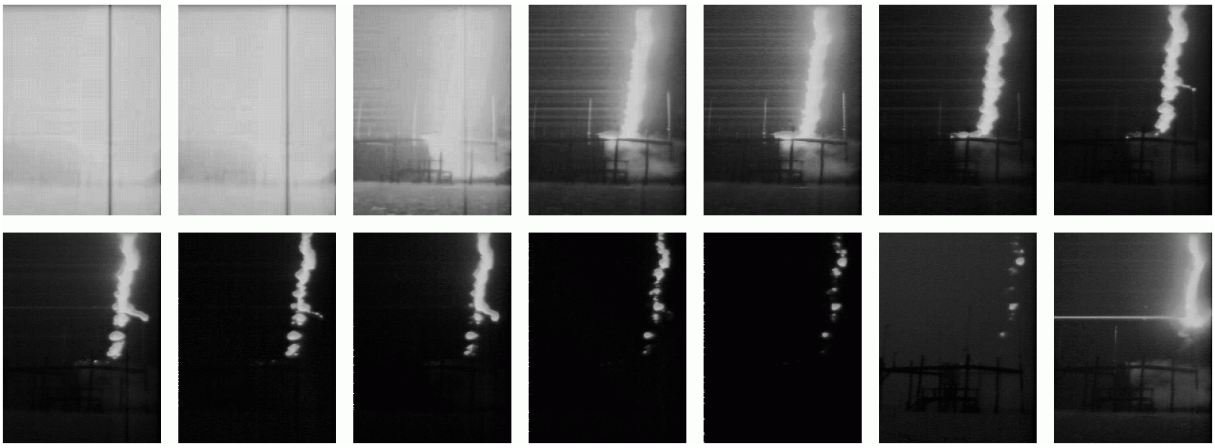

Figure 1: *Evolution of the beaded structure at 1 ms time intervals during a pause between the last two return strokes of a 10-stroke triggered lightning discharge.*

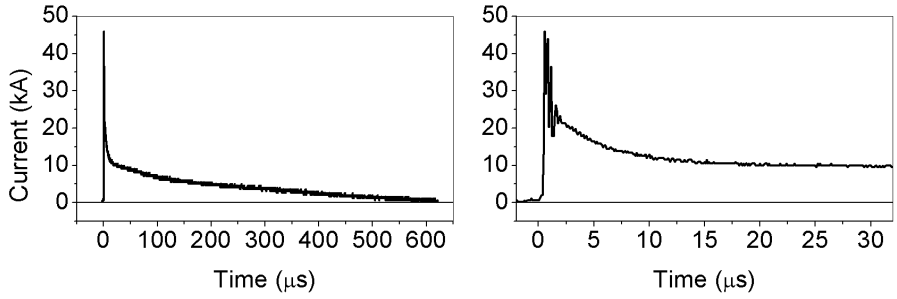

Figure 2: *Typical current waveform of a 45 kA return stroke in triggered lightning discharges shown for two different time scales.*

return stroke. These instabilities have a similar role in defining the beaded structure of the decaying return stroke. However, since the magnetic pressure is much smaller than the kinetic pressure, the hydromagnetic instabilities are much weaker than the hydrodynamic instability while the latter one lasts. Therefore, it is mainly the Rayleigh-Taylor instability that defines the final beaded structure [6].

As briefly discussed in the previous paragraph, the main source of instability in lightning is the transient acceleration at the channel boundary during the contraction stage. Hence, the magnetic field effects can be neglected in the simplified equation of motion (10)

$$-\rho\omega^2\overrightarrow{\xi} \cong \nabla\left(\overrightarrow{\xi}\cdot\nabla p+\gamma p\nabla\cdot\overrightarrow{\xi}\right)-\overrightarrow{g}\nabla\cdot\left(\rho\overrightarrow{\xi}\right), \tag{13}$$

as well as in the fluid continuity and pressure balance conditions

$$\begin{gathered}\left\langle\widehat{n}\cdot\overrightarrow{\xi}\right\rangle=0,\\ \left\langle-\gamma p\nabla\cdot\overrightarrow{\xi}-\overline{\rho}\,(a)\,\overrightarrow{\xi}\cdot\overrightarrow{g}+\underbrace{i2\omega\eta\widehat{n}\cdot\left(\nabla\overrightarrow{\xi}\right)\cdot\widehat{n}}_{\text{damping}}\right\rangle\cong 0.\end{gathered} \tag{14}$$

For an expanding discharge with a sharp boundary of radius a and uniform internal and

external pressures $p_{i,e}$, the equilibrium pressure balance is

$$p_i + \overline{\rho}\,(a)\, g L_g \cong p_e, \tag{15}$$

where L_g is the scale length of the radial acceleration profile with maximum value g. In the snowplow model the quantity $2\pi a L_g \overline{\rho}\,(a)$ gives the total mass inside the cylindrical shell of unit length, radius a, and thickness $L_g \ll a$. Viscosity of the external air is negligible, but viscosity effects inside the discharge are relevant because of the high temperature and expected turbulent fluctuations. The full dispersion relation for this problem becomes

$$\left(\frac{\rho_i I_m\left(\kappa_i a\right)}{\kappa_i I_m'\left(\kappa_i a\right)} - \frac{\rho_e K_m\left(\kappa_e a\right)}{\kappa_e K_m'\left(\kappa_e a\right)}\right)\omega^2 + 2\eta_i\left(\frac{\kappa_i I_m''\left(\kappa_i a\right)}{I_m'\left(\kappa_i a\right)}\right) i\omega - 2\overline{\rho}\,(a)\, g = 0, \tag{16}$$

where $\kappa_{i,e} a = \sqrt{k^2 a^2 - \omega^2 a^2 / c_{i,e}^2}$, and $c_{i,e}$ denotes the internal and external values of the speed of sound. The short wavelength limit gives

$$\left(\frac{\rho_e + \rho_i}{2\overline{\rho}\,(a)}\right)\omega^2 + \frac{\eta_i k^2}{\overline{\rho}\,(a)} i\omega - gk \cong 0, \tag{17}$$

which corresponds to gravity waves ($\omega \sim \sqrt{gk}$) damped by viscosity. In the case of a contraction ($g < 0$) the maximum growth rate and corresponding wave number in the short wavelength limit (17) are given by

$$i\omega_{\max} \cong \left(\frac{\overline{\rho}\,(a)^2\, g^2}{2\left(\rho_e + \rho_i\right)\eta_i}\right)^{1/3} \quad , \quad k_{\max} \cong \left(\frac{\overline{\rho}\,(a)\left(\rho_e + \rho_i\right)|g|}{4\eta_i^2}\right)^{1/3}. \tag{18}$$

This result shows that viscosity defines the scale of the most unstable perturbations.

As turbulence arises from the instability, the ratio of apparent to molecular viscosity is given by the Reynolds number $Re = \Delta v \ell / \nu_i$, where the velocity fluctuations and the scale length of turbulence are defined respectively by $\Delta v = K_1 c_i$ and $\ell = K_2 a$. The numerical coefficients K_1 and K_2 must be determined from experimental data or simulations, but should be of the order of unity for fully developed turbulence, that is, $K_1 \cong K_2 \cong 1$. For a lightning discharge with central temperature $T_i \cong 10,000\,\mathrm{K}$ (decaying stage) the kinematic viscosity is $\nu_i \cong 0.0060\,\mathrm{m^2/s}$ and the speed of sound is $c_i \cong 2.0\,\mathrm{km/s}$. The corresponding temperature at the edge of the channel is $T_i \cong 3,800\,\mathrm{K}$, with $\nu_i \cong 0.0012\,\mathrm{m^2/s}$ and $c_i \cong 1.24\,\mathrm{km/s}$. During the contraction stage the channel radius for a 45 kA peak current lightning discharge is $a \cong 4\,\mathrm{cm}$ and the peak acceleration is $|g| \cong 7.1 \times 10^4\,\mathrm{m/s^2}$ [6]. It follows that Reynolds numbers of the order of $Re \sim 10,000$ can be expected for the largest scale fluctuations. Figure (3) shows the normalized growth rate, $i\omega a / c_i$, versus the normalized wave number, ka, obtained from the full dispersion relation (16) for a 45 kA discharge. The plots clearly show the shift of the maximum growth rate to larger wavelengths when the Reynolds number increases.

Table (1) gives the maximum growth rate and corresponding wave number of the kink instability in a 45 kA discharge for $Re = 1$ (molecular viscosity) and $Re \sim 10,000$ (fully developed turbulence). The characteristic wavelength for the largest scale velocity fluctuations is $\sim 0.5\,\mathrm{m}$, in agreement with the observations. The following picture of the discharge evolution emerges. In the beginning of the contraction stage the "gravitational" acceleration is relatively strong, the Rayleigh-Taylor instability rises very fast and the turbulence sets in on the small length scale defined by classical viscosity. During the

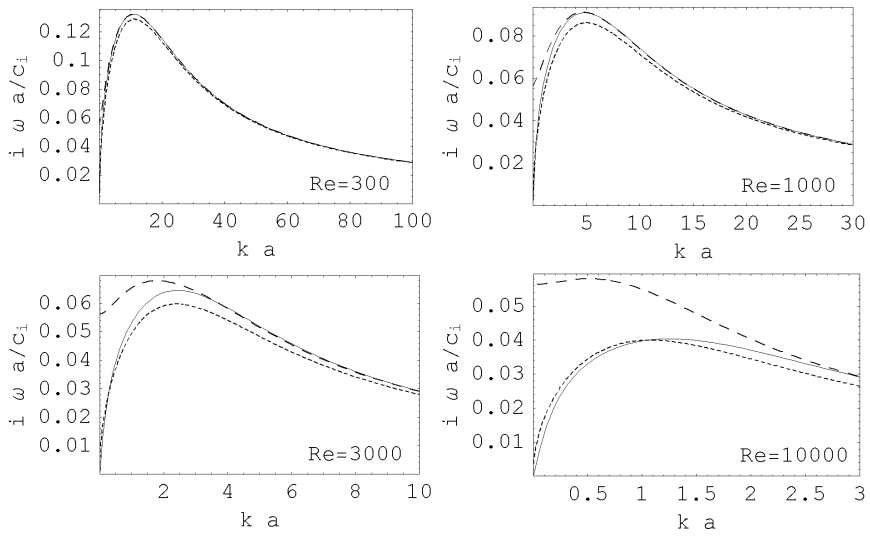

Figure 3: *Normalized growth rate of the Rayleigh-Taylor instability in a lightning discharge as a function of the normalized wave number for various values of the Reynolds number. The continuous line corresponds to the $m = 0$ sausage instability and the dashed line to the $m = 1$ kink instability. The short dashed line corresponds to the short wavelength asymptotic limit.*

contraction the turbulence develops, the large scale fluctuations fill the arc channel and the viscosity becomes strongly anomalous, shifting the wavelength of the most unstable modes to values of the order of and larger than the channel radius a. This process takes a few milliseconds, before the instability weakens and the spatial structure becomes frozen. From this point on one may conjecture that the discharge channel slowly diffuses before the turbulence decays in the absence of a driving energy source. The visible pictures (Fig. 1) correspond to a diffuse channel showing the frozen spatial structure of the instabilities during the history of their evolution. The main question is the actual level of turbulence reached in the discharge, a problem suitable to be investigated by simulation.

	Re=1	**Re=10,000**
$i\omega_{\max}a/c_i$	0.862 (37 μs)	0.0580 (0.55 ms)
$(ka)_{\max}$	500 (0.5 mm)	0.513 (49 cm)

Table 1: *Maximum growth rate and corresponding wave number of the kink instability in a 45 kA lightning discharge for extreme values of the Reynolds number.*

4. Laboratory plasma: high beta instabilities

The second example in this paper treats the effect of viscosity on the kink stability in a screw pinch. Only preliminary calculations are presented, dealing with the case of negligible flow. The equilibrium variables, which correspond to a sharp boundary plasma with a surface current $K_0 = I_0/(2\pi a)$, can be written in the form

$$\begin{aligned} r < a: \quad & p(r) = p_0, \\ & B_\theta(r) = 0, \\ & \frac{B_z^2(r)}{2\mu_0} = \frac{B_0^2}{2\mu_0} + \frac{\mu_0 I_0^2}{8\pi^2 a^2} - p_0. \end{aligned} \qquad \begin{aligned} r \geq a: \quad & p(r) = 0, \\ & B_\theta(r) = B_\theta(a)\frac{a}{r} = \frac{\mu_0 I_0}{2\pi r}, \\ & B_z(r) = B_z(a) = B_0. \end{aligned} \tag{19}$$

The simplified equation of motion (10), without acceleration effects, is

$$-\rho\omega^2\overrightarrow{\xi}-\frac{1}{\mu_0}\overrightarrow{B}\cdot\delta\overrightarrow{B}\cong-\nabla\delta p^*+\frac{1}{\mu_0}\delta\overrightarrow{B}\cdot\nabla\overrightarrow{B}, \tag{20}$$

and the boundary conditions are specified by the continuity of the magnetic field, fluid continuity, and normal pressure balance

$$\begin{gathered}\widehat{n}\cdot\left[\delta\overrightarrow{B}-\nabla\times\left(\overrightarrow{\xi}\times\overrightarrow{B}\right)\right]_a=0\quad\text{if}\quad\overrightarrow{K}\neq0,\\ \left\langle\widehat{n}\cdot\overrightarrow{\xi}\right\rangle=0,\\ \left\langle\delta p^*+\overrightarrow{\xi}\cdot\nabla p+\left(\overrightarrow{\xi}\cdot\nabla\right)\frac{B^2}{2\mu_0}+\underbrace{i2\omega\eta\widehat{n}\cdot\left(\nabla\overrightarrow{\xi}\right)\cdot\widehat{n}}_{\text{damping}}\right\rangle\cong0.\end{gathered} \tag{21}$$

Considering the perturbations as incompressible, that is, $\nabla\cdot\overrightarrow{\xi}=0$, and defining the Alfvén velocity $v_A=|B_z(a)|/\sqrt{\mu_0\rho}$ and the beta value

$$\beta=\frac{2\mu_0p_0}{B_z^2(a)+B_\theta^2(a)}=1-\frac{B_z^2(0)}{B_z^2(a)+B_\theta^2(a)}, \tag{22}$$

the dispersion relation for the surface current model becomes

$$\begin{aligned}\frac{a^2\omega^2}{v_A^2}-\underbrace{(1-\beta)\left(1+\frac{B_\theta^2(a)}{B_z^2(a)}\right)(ka)^2}_{\text{interior}}+\underbrace{\frac{kaI_m'(ka)}{I_m(ka)}\frac{B_\theta^2(a)}{B_z^2(a)}+2\frac{(ka)^2I_m''(ka)}{I_m(ka)}\frac{i\omega\eta}{\rho v_A^2}}_{\text{surface}}\\ +\underbrace{\frac{I_m'(ka)}{I_m(ka)}\frac{K_m(ka)}{K_m'(ka)}\left(ka+\frac{mB_\theta(a)}{B_z(a)}\right)^2}_{\text{vacuum}}=0.\end{aligned} \tag{23}$$

The propagation constant in a torus is $k=n/R$. Assuming $m>0$, the unstable modes occur for $n<0$ (the source of the instability is the parallel current I_0). Defining the safety factor $q=aB_z(a)/[RB_\theta(a)]$ and taking $n=-1$ for the most unstable case, the long wavelength limit of (23) for $m\geq1$ yields

$$\frac{a^2\omega^2}{v_A^2}+2m(m-1)\frac{i\omega\eta}{\rho v_A^2}-\underbrace{\left(\frac{(1-\beta)\left[q^2+(ka)^2\right]-m+(m-q)^2}{q^2}\right)}_{>0\text{ for stability}}(ka)^2\cong0. \tag{24}$$

The critical beta for instabilities of a circular cylindrical plasma is given by [2]

$$\beta<1-\frac{m-(m-q)^2}{q^2}, \tag{25}$$

which reduces to the Kruskal-Shafranov condition $q>2/(2-\beta)>1$ for stability of the kink mode ($m=1$). Now, the ion viscosity at the edge is calculated by the Braginskii formula $\eta_{i0}=0.96n_ik_BT_i\tau_i$ resulting in the following estimate for the viscous coefficient in (24)

$$\frac{\eta_{i0}}{n_im_iav_A}=\frac{6.06\times10^{-6}T_i^{5/2}}{a\sqrt{n_i}\,|B|\,\lambda_{ii}}, \tag{26}$$

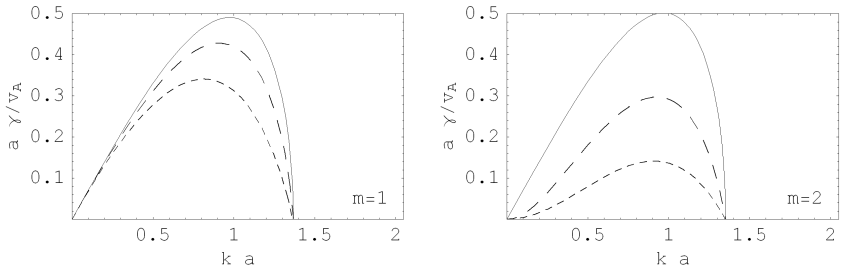

Figure 4: *Normalized growth rate versus normalized wave number of the high beta instabilities, for the poloidal mode numbers* $m = 1, 2$*, in a screw pinch with surface current. The continuous, dashed and short dashed lines correspond, respectively, to* $\eta_{i0}/(\rho a v_A) = 0$, 0.1 and 0.3.

with $k_B T_i/e = 10 \sim 100\,\mathrm{eV}$ and $n_i = 0.01 \sim 0.1 \times 10^{20}\,\mathrm{m}^{-3}$.

Figure (4) displays, for the poloidal mode numbers $m = 1$ and $m = 2$, the normalized growth rate, $a\gamma/v_A = ai\omega/v_A$, versus the normalized wave number, ka, of the high beta instabilities in a screw pinch with surface current (surface current model of a cylindrical tokamak). It is assumed $a = 1\,\mathrm{m}$, $B_0 = 1\,\mathrm{T}$, $q = 1$, and a large $\beta = 0.5$. The viscous term, which is proportional to the sheared velocity perturbation, reduces the growth rate, particularly of the high m-number instabilities.

In general terms, viscosity introduces damping of any sheared velocities. Hence, in the absence of flow (vorticity), viscosity damps out high mode number oscillations but does not change the plasma stability conditions. However, this result indicates that the balooning modes are affected by the interplay of viscosity and non-zero flow acting as a "surface tension" at the plasma edge. In the presence of flow, the viscous forces counteract the free-boundary perturbations, possibly modifying the beta limit for stability. Heating the plasma edge would increase the viscosity and change the confinement properties. With turbulence, the Reynolds number acts as an additional control parameter. The present topics of investigation involve equilibrium calculations, using boundary layer methods, of the vorticity layers that can be maintained at the edge by the balance between magnetic and viscous forces, and the analysis of their stability.

References

[1] LANDAU, L.D., LIFSHITZ, E.M. "Fluid Mechanics", Pergamon Press, Oxford, 1959.

[2] BATEMAN, G. "MHD Instabilities", MIT Press, Cambridge, MA, 1978.

[3] FREIDBERG, J.P. "Ideal Magnetohydrodynamics", Plenum, New York, 1987.

[4] RAKOV, V.A., UMAN, M.A. "Lightning - Physics and Effects", Cambridge University Press, Cambridge, MA, 2003, Chap. 20.

[5] LUDWIG, G.O., SABA, M.M.F., POTVIN, C. "Interchange instabilities in lightning discharges". In 30th EPS Conference on Controlled Fusion and Plasma Physics, Europhysics Conference Abstracts 27A, paper P-1.040 (4 pages), 2003.

[6] LUDWIG, G.O., SABA, M.M.F. "Bead lightning formation" (in preparation).